# ACTH Inhibits bTREK-1 $K^+$ Channels through Multiple cAMP-dependent Signaling Pathways

Haiyan Liu, Judith A. Enyeart, and John J. Enyeart

Department of Neuroscience, The Ohio State University College of Medicine and Public Health, Columbus, OH 43210

Bovine adrenal zona fasciculata (AZF) cells express bTREK-1 $K^+$ channels that set the resting membrane potential and function pivotally in the physiology of cortisol secretion. Inhibition of these $K^+$ channels by adrenocorticotropic hormone (ACTH) or cAMP is coupled to depolarization and $Ca^{2+}$ entry. The mechanism of ACTH and cAMP-mediated inhibition of bTREK-1 was explored in whole cell patch clamp recordings from AZF cells. Inhibition of bTREK-1 by ACTH and forskolin was not affected by the addition of both H-89 and PKI(6–22) amide to the pipette solution at concentrations that completely blocked activation of cAMP-dependent protein kinase (PKA) in these cells. The ACTH derivative, *O*-nitrophenyl, sulfenyl-adrenocorticotropin (NPS-ACTH), at concentrations that produced little or no activation of PKA, inhibited bTREK-1 by a $Ca^{2+}$-independent mechanism. Northern blot analysis showed that bovine AZF cells robustly express mRNA for Epac2, a guanine nucleotide exchange protein activated by cAMP. The selective Epac activator, 8-pCPT-2'-O-Me-cAMP, applied intracellularly through the patch pipette, inhibited bTREK-1 ($IC_{50}$ = 0.63 μM) at concentrations that did not activate PKA. Inhibition by this agent was unaffected by PKA inhibitors, including RpcAMPS, but was eliminated in the absence of hydrolyzable ATP. Culturing AZF cells in the presence of ACTH markedly reduced the expression of Epac2 mRNA. 8-pCPT-2'-O-Me-cAMP failed to inhibit bTREK-1 current in AZF cells that had been treated with ACTH for 3–4 d while inhibition by 8-br-cAMP was not affected. 8-pCPT-2'-O-Me-cAMP failed to inhibit bTREK-1 expressed in HEK293 cells, which express little or no Epac2. These findings demonstrate that, in addition to the well-described PKA-dependent TREK-1 inhibition, ACTH, NPS-ACTH, forskolin, and 8-pCPT-2'-O-Me-cAMP also inhibit these $K^+$ channels by a PKA-independent signaling pathway. The convergent inhibition of bTREK-1 through parallel PKA- and Epac-dependent mechanisms may provide for failsafe membrane depolarization by ACTH.

The Journal of General Physiology

## INTRODUCTION

Cortisol secretion from the adrenal zona fasciculata (AZF) occurs under the control of the pituitary peptide ACTH (adrenocorticotropic hormone) (Simpson and Waterman, 1988). The molecular mechanisms that couple ACTH receptor activation to cortisol production are only partially understood. Early studies established that cAMP was the principal intracellular messenger for ACTH in AZF cells (Haynes and Berthet, 1957; Grahame-Smith et al., 1967; Richardson and Schulster, 1973; Sala et al., 1979). ACTH stimulates cAMP synthesis in AZF cells, while cAMP mimics the steroidogenic actions of ACTH (Haynes et al., 1959; Roesler et al., 1988; Simpson and Waterman, 1988; Waterman, 1994). Accordingly, bovine AZF cells express a high affinity, MC2-R melanocortin receptor coupled to adenylate cyclase through $G_s$ (Penhoat et al., 1989; Raikhinstein et al., 1994).

Although cAMP appears to function as the primary intracellular messenger, $Ca^{2+}$ may also act pivotally in ACTH-stimulated corticosteroid secretion. At concentrations that produce little or no measurable increase in cAMP synthesis, ACTH has been reported to increase intracellular $Ca^{2+}$ concentration and stimulate cortisol secretion in bovine AZF cells (Yanagibashi et al., 1990; Kimoto et al., 1996). Similarly, the *O*-nitrophenyl, sulfenyl derivative of ACTH (NPS-ACTH) stimulates large increases in $[Ca^{2+}]_i$ and corticosteroid secretion at concentrations that trigger no measurable increases in cAMP synthesis in either rat or bovine AZF cells (Moyle et al., 1973; Yamazaki et al., 1998). Overall, these results suggest that cAMP and $Ca^{2+}$ are dual messengers that are both required to mediate the full steroidogenic response to ACTH.

In this regard, a role for electrical events and depolarization-dependent $Ca^{2+}$ entry in ACTH-stimulated cortisol secretion has been established (Enyeart et al., 1993; Mlinar et al., 1993). Specifically, bovine AZF cells express bTREK-1 leak-type $K^+$ channels, which set the resting membrane potential (Mlinar et al., 1993; Enyeart et al., 2002). ACTH receptor activation is coupled to membrane depolarization and $Ca^{2+}$ entry through the inhibition of bTREK-1 channels (Enyeart et al., 1993, 1996;

Correspondence to John J. Enyeart: enyeart.1@osu.edu

Abbreviations used in this paper: ACTH, adrenocorticotropic hormone; AngII, angiotensin II; AZF, adrenal zona fasciculata; BAPTA, 1,2 *bis*-(2-aminophenoxy)ethane-*N,N,N',N'*-tetraacetic acid; NPS-ACTH, *O*-nitrophenyl, sulfenyl-adrenocorticotropin.



The Rockefeller University Press $30.00
J. Gen. Physiol. Vol. 132 No. 2 279–294
www.jgp.org/cgi/doi/10.1085/jgp.200810003

Mlinar et al., 1993). Accordingly, organic $Ca^{2+}$ antagonists inhibit T-type $Ca^{2+}$ channels at concentrations that also inhibit ACTH-stimulated cortisol secretion (Enyeart et al., 1993). The NPS-ACTH–stimulated increase in $[Ca^{2+}]_i$ in bovine AZF cells is also inhibited by organic $Ca^{2+}$ antagonists at concentrations that inhibit T-type $Ca^{2+}$ channels (Yamazaki et al., 1998). Thus, bTREK-1 appears to link ACTH receptor activation to cortisol secretion through depolarization-dependent $Ca^{2+}$ entry.

The signaling mechanisms by which ACTH inhibits bTREK-1 channels are incompletely understood. They may involve multiple cAMP- and $Ca^{2+}$-dependent pathways. Specifically, neuronal TREK-1 channels are inhibited by cAMP through PKA-dependent phosphorylation of a carboxyl-terminal serine that is also present in bTREK-1 channels (Patel et al., 1998; Honoré, 2007). Although native bTREK-1 channels can also be inhibited by this mechanism, ACTH and cAMP inhibit bTREK-1 channels in AZF cells in the presence of any of several PKA antagonists (Enyeart et al., 1996).

While all of the cAMP-dependent actions of ACTH in AZF cells were previously thought to be mediated by PKA, alternative signaling pathways for cAMP-mediated responses are likely present in these cells. Specifically, two cAMP-activated guanine nucleotide exchange factors, Epac1 and Epac2 (also known as cAMP-GEFI and cAMP-GEFII), have been identified and implicated in the regulation of proteins including ion channels (de Rooij et al., 1998; Kawasaki et al., 1998; Holz et al., 2008). While Epac1 is expressed in many tissues, Epac2 is robustly expressed in selected areas of the brain and the adrenal glands of rats and humans (Kawasaki et al., 1998). This raises the possibility that cAMP-dependent inhibition of bTREK-1 in the adrenal gland is mediated through separate PKA- and Epac2-dependent mechanisms.

In addition, studies with NPS-ACTH raise the possibility that ACTH might inhibit bTREK-1 by a $Ca^{2+}$-dependent mechanism that is independent of both cAMP and PKA. In this regard, angiotensin II (AngII) which also stimulates cortisol secretion from bovine AZF cells, inhibits bTREK-1 in these cells by separate $Ca^{2+}$- and ATP-dependent pathways (Gomora and Enyeart, 1998; Enyeart et al., 2005; Liu et al., 2007). Overall, our results and those of other investigators suggest that ACTH may regulate bTREK-1 channels by multiple cAMP- and $Ca^{2+}$-dependent pathways.

In this regard, Epac1 and Epac2 possess cAMP binding domains that lack a specific glutamate residue present in the binding domain of PKA (Enserink et al., 2002). Using this information and rational drug design, novel cAMP analogues were developed that, at appropriate concentrations, selectively activate the Epac proteins (Enserink et al., 2002; Christensen et al., 2003). We have used one of these, 8-pCPT-2'-O-Me-cAMP, along with other agents involved in cAMP metabolism to further characterize the signaling pathways by which ACTH and cAMP inhibit bTREK-1 in bovine AZF cells. The goal of this study was to determine whether ACTH and cAMP could inhibit bTREK-1 by Epac2 as well as PKA-dependent pathways.

Some of these results have been reported in abstract form (H. Liu, J.A. Enyeart, and J.J. Enyeart. 2008. *Biophys. J.* 94:2181).

## MATERIALS AND METHODS

### Materials

Tissue culture media, antibiotics, fibronectin, and FBS were obtained from Invitrogen. Coverslips were from Bellco. PBS, enzymes, 1,2 *bis*-(2-aminophenoxy)ethane-*N,N,N',N'*-tetraacetic acid (BAPTA), MgATP, collagenase, DNase, H-89, nystatin, 8-pCPT-cAMP, and ACTH (1–24), AMP-PNP, and Rp-cAMPS were obtained from Sigma-Aldrich. PKI(6–22) amide and PKI(14–22)myristolated were purchased from EMD Biosciences, Inc. 8-pCPT-2'-O-Me-cAMP (Biolog #C041) was purchased from Axxora, LLC. Human full-length cDNA for Epac2 (cAMP-GEFII, clone ID# 4823935) was purchased from Open Biosystems. p3-CD8 clone was provided by B. Seed (Massachusetts General Hospital, Boston, MA). SignaTect cAMP-dependent protein kinase (PKA) assay system was from Promega. [$\gamma^{32}$P] ATP was purchased from Perkin Elmer. NPS-ACTH was custom synthesized by Celtek Peptides.

### Isolation and Culture of AZF Cells

Bovine adrenal glands were obtained from steers (age 2–3 yr) at a local slaughterhouse. Isolated AZF cells were obtained and prepared as previously described (Enyeart et al., 1997). After isolation, cells were either resuspended in DMEM/F12 (1:1) with 10% FBS, 100 U/ml penicillin, 0.1 mg/ml streptomycin, and the antioxidants α-tocopherol (1 μM), 20 nM selenite, and 100 μM ascorbic acid (DMEM/F12+) and plated for immediate use, or resuspended in FBS/5% DMSO, divided into 1 ml aliquots, and stored in liquid nitrogen for future use. To ensure cell attachment, dishes were treated with fibronectin (10 μg/ml) at 37°C for 30 min and then rinsed with warm, sterile PBS immediately before adding cells. For patch clamp experiments, cells were plated in DMEM/F12+ in 35-mm dishes containing 9-$mm^2$ glass coverslips. Coverslips were treated with fibronectin (10 μg/ml) as described above. Cells were maintained at 37°C in a humidified atmosphere of 95% air–5% $CO_2$.

### Measurement of Epac2 mRNA

RNeasy columns (QIAGEN) that had been treated with RNase-free DNase (QIAGEN) to remove genomic contamination were used to extract total RNA from AZF cells that had been cultured for 48 h both with and without ACTH (2 nM) or confluent HEK293 cells. Poly(A)$^+$ mRNA was extracted from total RNA using a Poly(A) Pure kit (Ambion). 7 μg of total or poly(A)$^+$ mRNA were separated on a denaturing 8% formaldehyde, 1.0% agarose gel, and transferred to a nylon membrane (Gene Screen Plus, NEN). The RNA was fixed to the membrane by UV cross-linking using a Stratalinker (Stratagene). Northern blots were prehybridized in heat-sealable plastic bags for 2 h at 42°C in ULTRAhyb (Ambion) and then hybridized with a [α $^{32}$P]dCTP-labeled 700-bp *XHO1* fragment of h-Epac2 DNA overnight at 42°C in minimal volume of ULTRAhyb. After 18–24 h, membrane was washed twice at room temperature in 2× SSPE for 15 min, twice at 40°C in 1× SSPE, 1% SDS for 30 min, with a final wash at 40°C with 0.1× SSPE, 1% SDS for 15 min before exposing to a storage phosphor screen for 4–12 h. Northern autoradiogram was imaged using a Typhoon 9200 variable mode phosphorimager.

### Patch Clamp Experiments

Patch clamp recordings of $K^+$ channel currents were made in the whole cell and perforated patch configurations from bovine AZF cells. The standard external solution consisted of 140 mM NaCl, 5 mM KCl, 2 mM $CaCl_2$, 2 mM $MgCl_2$, 10 mM HEPES, and 5 mM glucose, with pH adjusted to 7.3 using NaOH. The standard pipette solution consisted of 120 mM KCl, 1 mM $CaCl_2$, 2 mM $MgCl_2$, 11 mM BAPTA, 10 mM HEPES, 5 mM ATP, and 200 μM GTP, with pH titrated to 6.8 using KOH. The buffering capacity of pipette solutions was varied by adding combinations of $CaCl_2$ and BAPTA or EGTA using the Bound and Determined software program (Brooks and Storey, 1992). Low and high capacity $Ca^{2+}$ buffering solutions contained 0.5 mM EGTA and 11 mM BAPTA, respectively. The low capacity $Ca^{2+}$ buffering solution was nominally $Ca^{2+}$ free. $[Ca^{2+}]_i$ was buffered to 22 nM in the high capacity buffering solution. The patch pipette solution was maintained at pH 6.8 to enhance the expression of bTREK-1. For perforated patch recordings, the pipette solution contained 130 mM KCl, 2 mM $MgCl_2$, and 20 mM HEPES, with pH adjusted to 6.8 using KOH. The pipette tip was filled with this solution and backfilled with this same solution supplemented with 120 μg/ml nystatin. Nystatin stock solutions (30 mg/ml) were made fresh daily in DMSO. Perforated patch recordings were made as previously described (Horn and Marty, 1988).

### Recording Conditions and Electronics

AZF cells were used for patch clamp experiments 2–12 h after plating. Typically, cells with diameters <15 μm and capacitances of 10–15 pF were selected. Coverslips were transferred from 35-mm culture dishes to the recording chamber (volume: 1.5 ml) that was continuously perfused by gravity at a rate of 3–5 ml/min. For whole cell recordings, patch electrodes with resistances of 1.0–2.0 MΩ were fabricated from Corning 0010 glass (World Precision Instruments). These electrodes routinely yielded access resistances of 1.5–4.0 MΩ and voltage-clamp time constants of <100 μs. $K^+$ currents were recorded at room temperature (22–25°C) according to the procedure of Hamill et al. (1981) using a List EPC-7 patch clamp amplifier.

Pulse generation and data acquisition were done using a personal computer and PCLAMP software with Digidata 1200 interface (Axon Instruments, Inc.). Currents were digitized at 2–10 kHz after filtering with an 8-pole Bessel filter (Frequency Devices). Linear leak and capacity currents were subtracted from current records using summed scaled hyperpolarizing steps of 1/2 to 1/4 pulse amplitude. Data were analyzed using CLAMPFIT 9.2 (Molecular Devices) and SigmaPlot (version 10.0) software. Drugs were applied by bath perfusion, controlled manually by a six-way rotary valve.

### PKA Assay

PKA activity was measured with a SignaTECT cAMP-dependent protein kinase assay kit (Promega). This kit uses PKA-dependent phosphorylation of biotinylated peptides as a measure of PKA activity. AZF cells were plated on 60-mm fibronectin-treated dishes in DMEM/F12+ at a density of $\sim 4 \times 10^6$ cells/dish. After 24 h, the serum-supplemented media was removed and replaced with either control media (DMEM/F12+) or the same media containing myristolyated PKI(14–22) and H-89. At the end of the incubation period, cells were washed two times with ice-cold PBS and suspended in 500 μl of cold extraction buffer (25 mM Tris-HCl pH 7.4, 0.5 mM EGTA, 10 mM β-mercaptoethanol, 0.5 mM Pefabloc-SC [Roche Applied Science], and protease inhibitors with EDTA [Complete Mini protease inhibitor cocktail tablet, 1 per 10 ml lysis solution, Roche Applied Science]). Lysates were homogenized using a cold Dounce homogenizer then centrifuged for 5 min at 4°C at 14,000 *g*. 5-μl samples of lysate supernatant were assayed using the SignaTECT cAMP-dependent protein kinase assay system. Each experimental condition was assayed in quadruplicate.

### Transient Transfection and Visual Identification of HEK293 Cells Expressing bTREK-1

For patch clamp recording of bTREK-1 currents, HEK293 cells were cotransfected with a mixture of pCR®3.1-Uni-bTrek-1 and an expression plasmid (p3-CD8) for the α subunit of the human CD8 lymphocyte surface antigen at a 5:1 ratio using Lipofectamine (Life Technologies). Cells were visualized 1–2 d post transfection after a 15-min incubation with anti-CD8 antibody-coated beads (Dynal Biotech Inc.) as previously described (Jurman et al., 1994).

## RESULTS

Bovine AZF cells express two types of $K^+$ channels: a voltage-gated, rapidly inactivating Kv1.4 channel, and a two pore domain, four transmembrane-spanning segment (2P/4TMS) bTREK-1 background $K^+$ channel (Mlinar and Enyeart, 1993; Mlinar et al., 1993; Enyeart et al., 2000; Enyeart et al., 2002). In whole cell patch clamp recordings, bTREK-1 amplitude typically increases with time to a steady-state maximum. The absence of time- and voltage-dependent inactivation allows bTREK-1 $K^+$ currents to be isolated in whole cell recordings using either of two voltage clamp protocols. When voltage steps of several hundred milliseconds duration are applied from a holding potential of −80 mV, bTREK-1 $K^+$ current can be measured near the end of a voltage step when the Kv1.4 $K^+$ current has fully inactivated (Fig. 1, A–C, left traces). Alternatively, bTREK-1 current can be selectively activated by an identical voltage step applied immediately after a 10-s prepulse to −20 mV has fully inactivated Kv1.4 channels (Fig. 1, A–C, right traces).

In whole cell recordings from bovine AZF cells, we previously showed that ACTH inhibits bTREK-1 current by a mechanism that was insensitive to PKA antagonists H-89 and a synthetic inhibitory peptide PKI(5–24) when either was added to the recording pipette (Enyeart et al., 1996). This result indicated that ACTH could inhibit bTREK-1 by a PKA-independent pathway. In the present study, we measured the inhibition of bTREK-1 with the addition of a second PKI inhibitory peptide, PKI(6–22) amide, to the pipette solution, either alone or in combination with H-89. PKI(6–22) amide is a synthetic peptide patterned after a portion of the naturally occurring PKA inhibitory peptide and inhibits PKA with a reported $IC_{50}$ of 1.7 nM (Glass et al., 1989). When added to cytoplasmic extracts from AZF cells, PKI(6–22) amide (4 μM) and H-89 (10 μM) completely inhibited PKA activated by maximally effective concentrations of cAMP (see Fig. 7 C).

In contrast, when applied directly to the cytoplasm of AZF cells through the patch electrode, these PKA inhibitors failed to alter the potency or effectiveness of ACTH as an inhibitor of bTREK-1. ACTH inhibits bTREK-1 with an $IC_{50}$ of 4.1 pM (Mlinar et al., 1993). With standard pipette solution, ACTH (200 pM) inhibited bTREK-1 almost completely (95.2 ± 2.4%, $n = 4$) (Fig. 1, A and D). The addition of PKI(6–22) amide (2 or 4 μM) to the

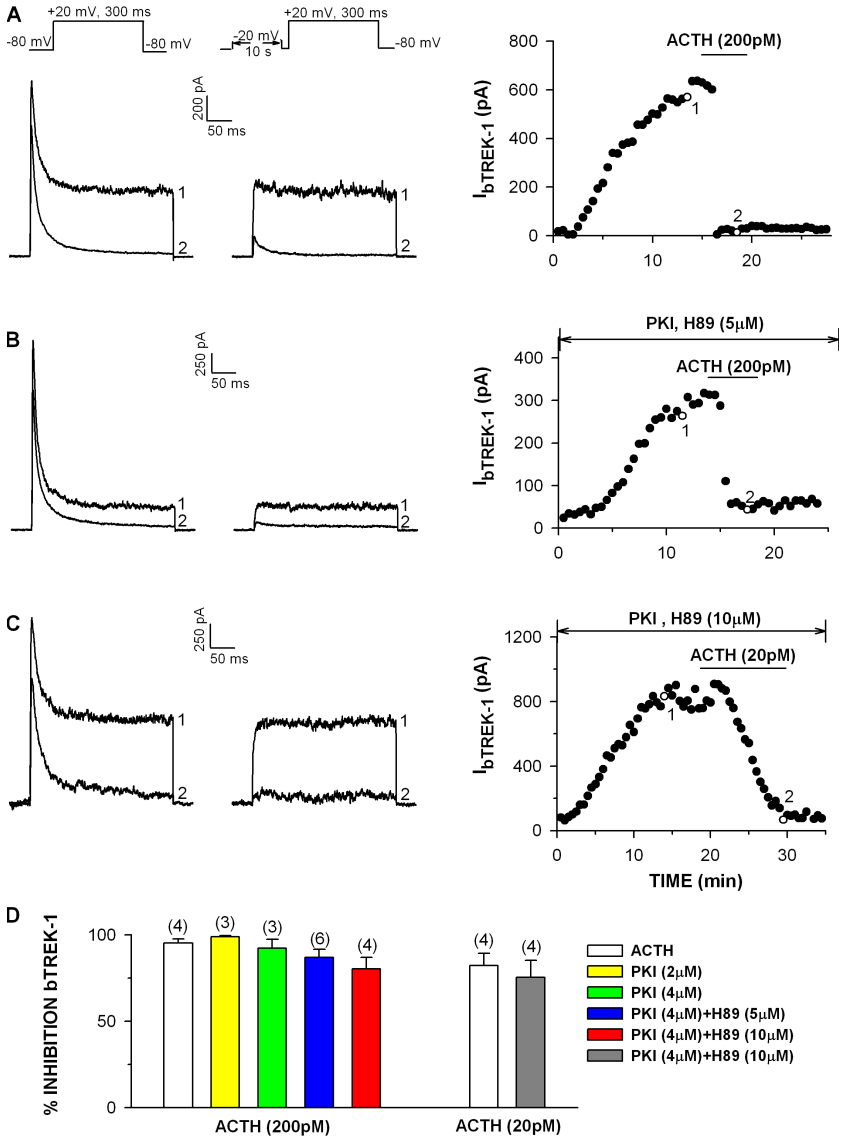


**Figure 1.** Effect of PKA inhibitors on bTREK-1 inhibition by ACTH. Whole cell $K^+$ currents were recorded from AZF cells in response to voltage steps applied from −80 mV at 30-s intervals with or without depolarizing prepulses to −20 mV. Pipettes contained standard solution or the same solution supplemented with PKI(6–22) amide (2 or 4 μM) alone or in combination with H-89 (5 or 10 μM). After bTREK-1 reached a stable maximum, cells were superfused with ACTH (1–24) (200 pM). (A–C) $K^+$ current traces recorded with (right traces) and without (left traces) depolarizing prepulses, and corresponding plot of bTREK-1 amplitudes with (open circles) and without (closed circles) depolarizing pulses. Numbers on traces correspond to those on plots. (D) Summary of experiments as in A–C. Bars indicate mean ± SEM of bTREK-1 inhibition by 20 or 200 pM ACTH with or without PKA inhibitors as indicated.

pipette solution did not blunt ACTH-induced inhibition of bTREK-1 (Fig. 1 D). PKI(6–22) amide in combination with H-89 (5 or 10 μM) also failed to significantly reduce ACTH-mediated inhibition of bTREK-1 (Fig. 1, B and D). The PKA inhibitors were also ineffective at reducing bTREK-1 inhibition by ACTH at a concentration of 20 pM where <2% of all receptors would be activated (Buckley and Ramachandran, 1981; Raikhinstein et al., 1994) (Fig. 1, C and D).

### bTREK-1 Inhibition by ACTH and cAMP Is Voltage Independent

These results provide further proof that ACTH inhibits bTREK-1 by a PKA-independent mechanism. In this regard, cAMP acting through PKA was reported to inhibit hippocampal TREK-1 channels by a mechanism that converted TREK-1 from a voltage-insensitive leak channel into a voltage-gated outward rectifier (Bockenhauer et al., 2001). When phosphorylated by PKA, TREK-1 channel open probability was markedly reduced only at negative potentials.

To determine whether ACTH or cAMP converted native bTREK-1 channels into voltage-gated channels, we measured bTREK-1 inhibition by ACTH (200 pM) or the membrane-permeable cAMP analogue 8-pCPT-cAMP over a wide range of test potentials. When bTREK-1 was activated by voltage steps between −60 and +40 mV, ACTH selectively inhibited this current almost completely at every test potential (Fig. 2 A). Similarly, when bTREK-1 currents were measured in response to voltage ramps between −100 and +100 mV, ACTH totally inhibited this current, even at the most positive test potential (Fig. 2 A).

In similar experiments, the membrane-permeable cAMP analogue 8-pCPT-cAMP (300 μM) inhibited bTREK-1 with equal effectiveness over the same range of test voltages (Fig. 2 B). These results indicate that neither ACTH nor cAMP inhibit bTREK-1 solely by converting it to a voltage-gated channel through PKA phosphorylation.

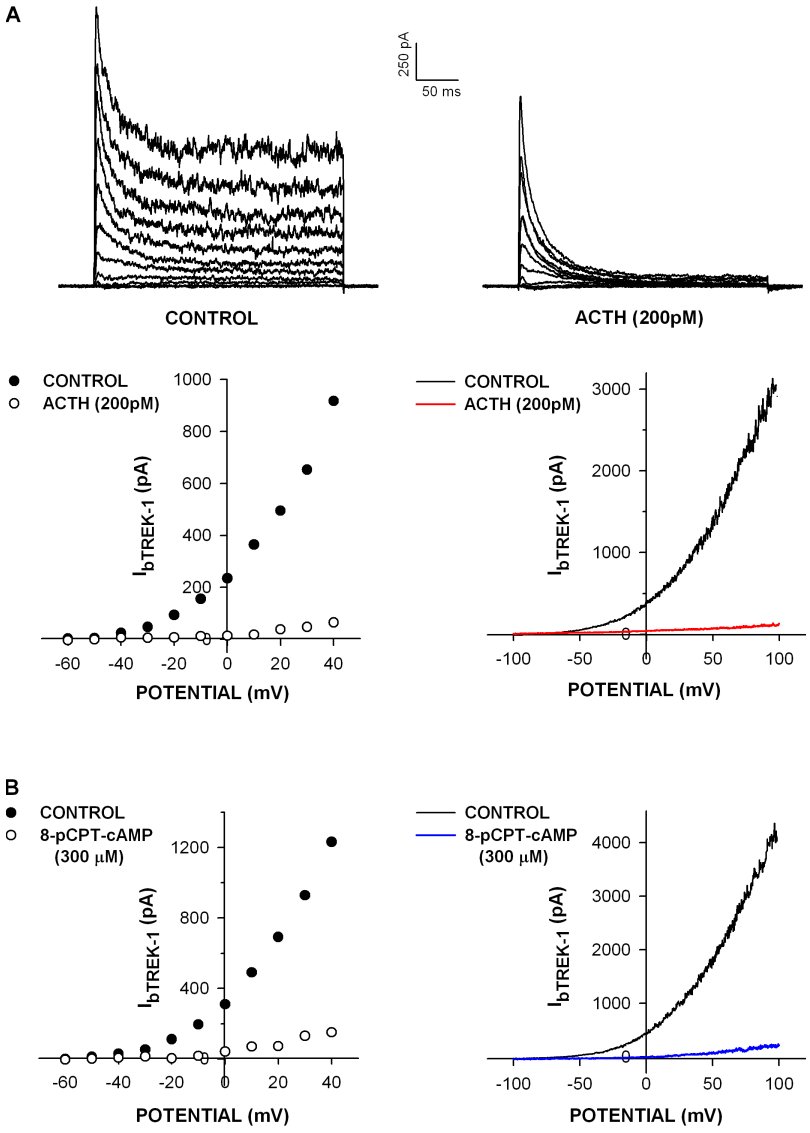


**Figure 2.** bTREK-1 inhibition by ACTH and 8-pCPT-cAMP is voltage independent. bTREK-1 was permitted to grow to a stable maximum before whole cell $K^+$ currents were activated in response to voltage steps or voltage ramps before and after superfusion of ACTH or 8-pCPT-cAMP. Voltage steps were applied at 30-s intervals in 10-mV increments from a holding potential of −80 mV to test potentials from −60 to +40 mV. Voltage ramps were applied at 100 mV/s to potentials between +100 and −100 mV from a holding potential of 0 mV. (A) Effect of ACTH: $K^+$ currents were recorded in response to voltage steps or voltage ramps before and after steady-state block by ACTH (200 pM). Top: current traces in response to voltage steps before and after ACTH. Bottom left: bTREK-1 amplitudes plotted against test potential before (closed circles) and after (open circles) ACTH. Bottom right: bTREK-1 current traces in response to ramp voltages before and after ACTH. (B, left) bTREK-1 amplitudes plotted against test potential in control saline (closed circles) and after 8-pCPT-cAMP (open circles). (B, right) bTREK-1 current traces in response to ramp voltages before and after 8-pCPT-cAMP.

Overall, these findings are consistent with the hypothesis that ACTH inhibits bTREK-1 through separate PKA-dependent and -independent mechanisms.

### NPS-ACTH Inhibits bTREK-1 by a PKA- and $Ca^{2+}$-independent Mechanism

Although our results are consistent with a model wherein ACTH inhibits bTREK-1 through parallel cAMP-dependent paths, they do not exclude the possibility that inhibition could also occur through a separate $Ca^{2+}$-dependent mechanism.

NPS-ACTH reportedly increases $[Ca^{2+}]_i$ in bovine AZF cells with little or no increase in cAMP synthesis (Yamazaki et al., 1998). This peptide was used to determine if ACTH could inhibit bTREK-1 by a $Ca^{2+}$-dependent pathway that is independent of cAMP. In this regard, AngII inhibits bTREK-1 by parallel $Ca^{2+}$- and ATP hydrolysis–dependent signaling pathways that can be activated separately using two different pipette solutions (Enyeart et al., 2005; Liu et al., 2007). The standard pipette solution containing 5 mM MgATP with $Ca^{2+}$ strongly buffered by 11 mM BAPTA facilitates selective activation of an ATP hydrolysis-dependent pathway. The $Ca^{2+}$-dependent pathway can be selectively activated with a pipette solution containing UTP instead of ATP, and 0.5 mM EGTA instead of 11 mM BAPTA (Enyeart et al., 2005).

It was discovered that NPS-ACTH inhibited bTREK-1 only through an ATP hydrolysis–dependent pathway. With pipette solution designed to permit selective activation of a $Ca^{2+}$-dependent pathway, NPS-ACTH (1 nM) failed to significantly inhibit bTREK-1. In contrast, AngII (10 nM) in these same experiments inhibited bTREK-1 by 72.1 ± 4.2% ($n = 3$) (Fig. 3 A). With pipette solution that allowed selective activation of the ATP-dependent pathway, NPS-ACTH reversibly and completely inhibited bTREK-1 with an $IC_{50}$ of 20.0 pM (Fig. 3, B and C).

These results suggested that NPS-ACTH may inhibit bTREK-1 by the same pathways as ACTH, although less

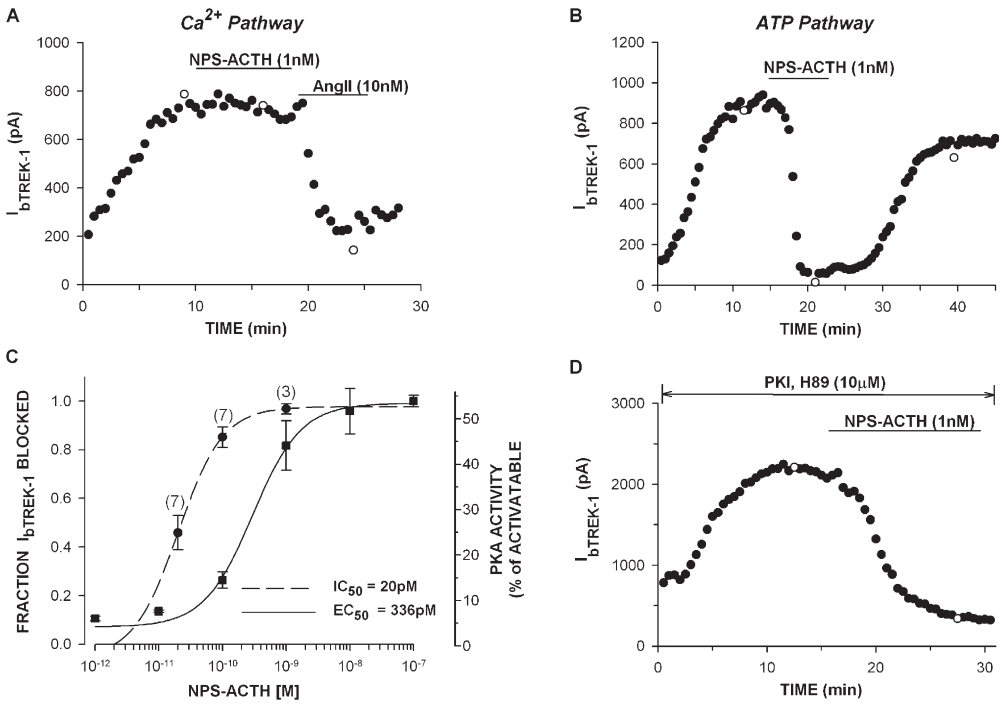


**Figure 3.** Inhibition of bTREK-1 by NPS-ACTH is $Ca^{2+}$ and PKA independent. The inhibition of bTREK-1 in bovine AZF cells by NPS-ACTH was measured in whole cell patch clamp recordings using pipette solutions that permitted or blocked activation of $Ca^{2+}$, ATP, or PKA-dependent signaling. $K^+$ currents were recorded at 30-s intervals in response to voltage steps to +20 mV from a holding potential of −80 mV. After currents reached a stable maximum, cells were superfused with NPS-ACTH. (A and B) Effect of NPS-ACTH on bTREK-1 through $Ca^{2+}$- and ATP hydrolysis–dependent pathways. bTREK-1 current amplitudes with (open circles) and without (closed circles) depolarizing prepulses are plotted against time. Pipette solutions contained (A) 2 mM UTP, 0.5 mM EGTA, (B) 5 mM MgATP, 11 mM BAPTA. NPS-ACTH and AngII were superfused at indicated times. (C) Concentration dependence of bTREK-1 inhibition and PKA activation by NPS-ACTH were measured in AZF cells and cell, respectively. Data were fit with an equation of the form (dotted line) $I/I_{MAX} = 1/[1 + (X/IC_{50})^B]$, where X is the NPS-ACTH concentration, and B is the Hill coefficient. $IC_{50}$ is the concentration that reduces bTREK-1 by 50%. Values are mean ± SEM of indicated number of determinations, (solid line) PKA activity = $1/[1+(X/EC_{50})^B]$, where X is the NPS-ACTH concentration, and B is the Hill coefficient. $EC_{50}$ is the concentration that produces 1/2 of the maximum response. (D) Effect of PKA inhibitors on NPS-ACTH inhibition of bTREK-1. bTREK-1 current amplitudes are plotted against time. Pipette solution contained PKI(6–22)amide (4 μM) and H-89 (10 μM).

potently. In this regard, the activation of PKA by ACTH in AZF cells serves as a remarkably sensitive measure of cAMP synthesis. In bovine AZF cells, ACTH activates PKA with an $EC_{50}$ of 1.4 pM (Enyeart and Enyeart, 1998). We found that NPS-ACTH activated PKA in AZF cells, but much less potently, with an $EC_{50}$ of 336 pM (Fig. 3 C). Although less potent than ACTH, NPS-ACTH was equally effective as a PKA activator at maximum concentrations (unpublished data).

These results show that NPS-ACTH increases cAMP synthesis in AZF cells to a level sufficient to activate PKA. However, they also indicate that bTREK-1 inhibition by NPS-ACTH occurs at concentrations that produce minimal activation of PKA. Accordingly, we found that bTREK-1 inhibition by NPS-ACTH was not affected by including PKA inhibitors in the patch pipette (Fig. 3 D). Overall, these experiments showed that NPS-ACTH increases cAMP synthesis in AZF cells, but can inhibit bTREK-1 by a PKA- and $Ca^{2+}$-independent mechanism.

### Forskolin Inhibits bTREK-1 by a PKA-independent Mechanism

Although all of the actions of ACTH in the adrenal cortex may require the synthesis of cAMP, the failure of PKA inhibitors to suppress bTREK-1 inhibition by ACTH could be indicative of a cAMP-independent, rather than a PKA-independent, action of cAMP. The di-terpene forskolin directly activates adenylate cyclase, increasing intracellular cAMP (Awad et al., 1983). If cAMP inhibits bTREK-1 in AZF cells solely through activation of PKA, then including PKA inhibitors in the recording pipette should block bTREK-1 inhibition by forskolin. Under control conditions, forskolin (2.5 μM) inhibited bTREK-1 current by 76.9 ± 9.3% ($n = 4$) (Fig. 4 A). The addition of PKI(6–22) amide and H-89 to the pipette solution, at concentrations that completely inhibited PKA, failed to significantly reduce bTREK-1 inhibition by forskolin (Fig. 4, B and C). These findings are consistent with the hypothesis that ACTH and cAMP inhibit bTREK-1 by the same PKA-independent mechanism.

### Effect of 8-pCPT-2′-O-Me-cAMP on PKA Activity and bTREK-1 Current in Perforated Patch Recordings

8-pCPT-2′-O-Me-cAMP has been reported to be a relatively selective activator of Epac proteins. It binds to Epac1 with 100-fold higher affinity than the cyclic nucleotide binding domain of the PKA regulatory subunit (Enserink et al., 2002; Christensen et al., 2003). When applied to cells in culture at concentrations up to 100 μM,

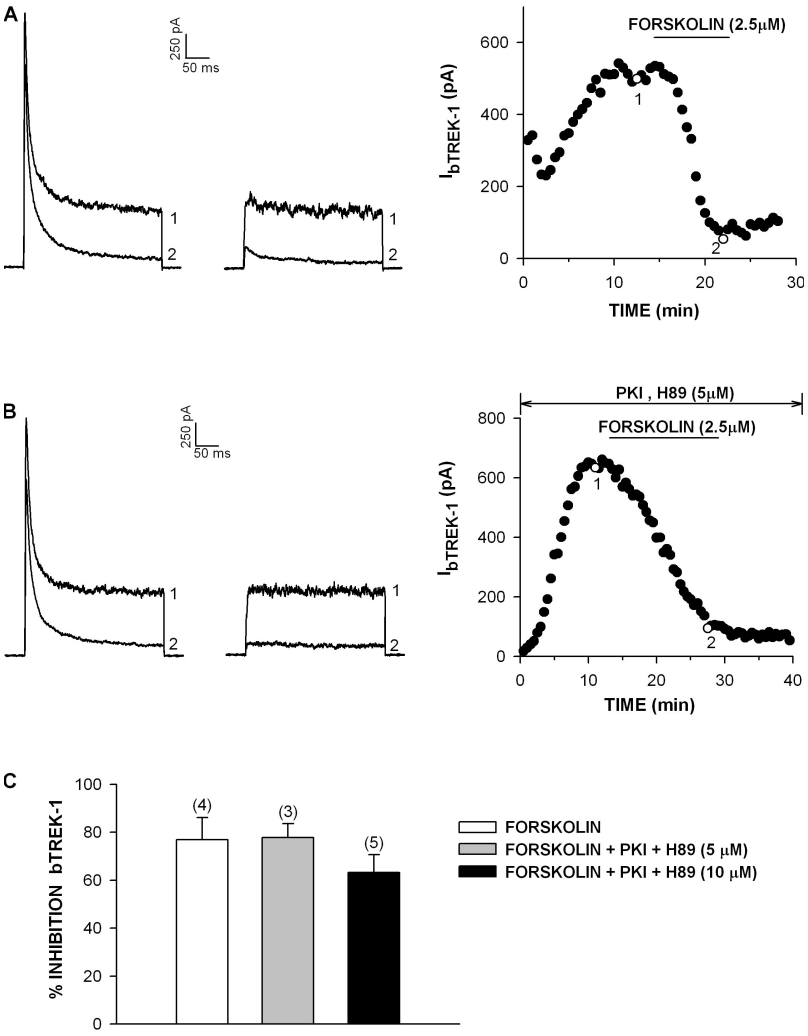


**Figure 4.** Effect of PKA inhibitors on bTREK-1 inhibition by forskolin. Whole cell $K^+$ currents were recorded from AZF cells in response to voltage steps applied from −80 mV at 30-s intervals with or without 10-s depolarizing prepulses to −20 mV. Patch pipettes contained standard solution or the same solution supplemented with PKI(6–22) amide (4 μM) alone or in combination with H-89 (5 or 10 μM). After bTREK-1 current reached a stable maximum, cells were superfused with forskolin (2.5 μM). (A and B) $K^+$ current traces recorded with (right traces) and without (left traces) prepulses, and corresponding plot of bTREK-1 amplitudes with (open circles) or without (closed circles) depolarizing pulses. Numbers on traces correspond to those on plots. (C) Summary of experiments as in A and B. Bars indicate mean ± SEM of bTREK-1 inhibition by forskolin (2.5 μM) with or without PKA inhibitors, as indicated.

8-pCPT-2'-O-Me-cAMP has been reported to activate Epac1, but not PKA (Enserink et al., 2002). However, in experiments on bovine AZF cells, we found that at concentrations >30 μM, 8-pCPT-2'-O-Me-cAMP produced significant increases in PKA activity. When applied externally at 100 μM, this cAMP analogue increased PKA activity approximately threefold over the control value (unpublished data).

These PKA activity measurements demonstrated that 8-pCPT-2'-O-Me-cAMP could be used in bovine AZF cells as a selective Epac activator at concentrations up to 30 μM. To determine whether 8-pCPT-2'-O-Me-cAMP could inhibit bTREK-1 independently of PKA, AZF cells were superfused with this agent while recording bTREK-1 currents with the nystatin perforated patch technique (Horn and Marty, 1988). By using this technique, we hoped to minimize cell dialysis allowing 8-pCPT-2'-O-Me-cAMP to reach a higher intracellular concentration. However, in these experiments, 8-pCPT-2'-O-Me-cAMP (30 μM) inhibited bTREK-1 by only 10.2 ± 6.4% ($n = 5$), while ACTH (200 pM) inhibited bTREK-1 under the same conditions by 83.8 ± 2.8% ($n = 7$) (Fig. 5, A and C).

The ineffectiveness of 8-pCPT-2'-O-Me-cAMP in perforated patch recordings suggested that ACTH and cAMP do not inhibit bTREK-1 through activation of Epac2. However, the membrane-permeable cAMP analogue 8-pCPT-cAMP, which potently activates PKA and Epac2 (Christensen et al., 2003), also failed to inhibit bTREK-1 when applied at a concentration of 30 μM in perforated patch recordings (Fig. 5, B and C). In contrast, at 10-fold higher concentrations, 8-pCPT-cAMP inhibited bTREK-1 by 91.2 ± 6.7 ($n = 3$) (Fig. 5, B and C). These findings indicate that even in perforated patch recordings, cyclic nucleotides applied externally fail to reach intracellular concentrations that are comparable to those present in the bath solution.

### Inhibition of bTREK-1 by Intracellular Application of 8-pCPT-2′-O-Me-cAMP

Because of the limited effectiveness of the cAMP analogues when applied extracellularly at low concentrations and the associated uncertainty of their intracellular concentrations, we measured the effects of 8-pCPT-2'-O-Me-cAMP on bTREK-1 $K^+$ channel activity when it was

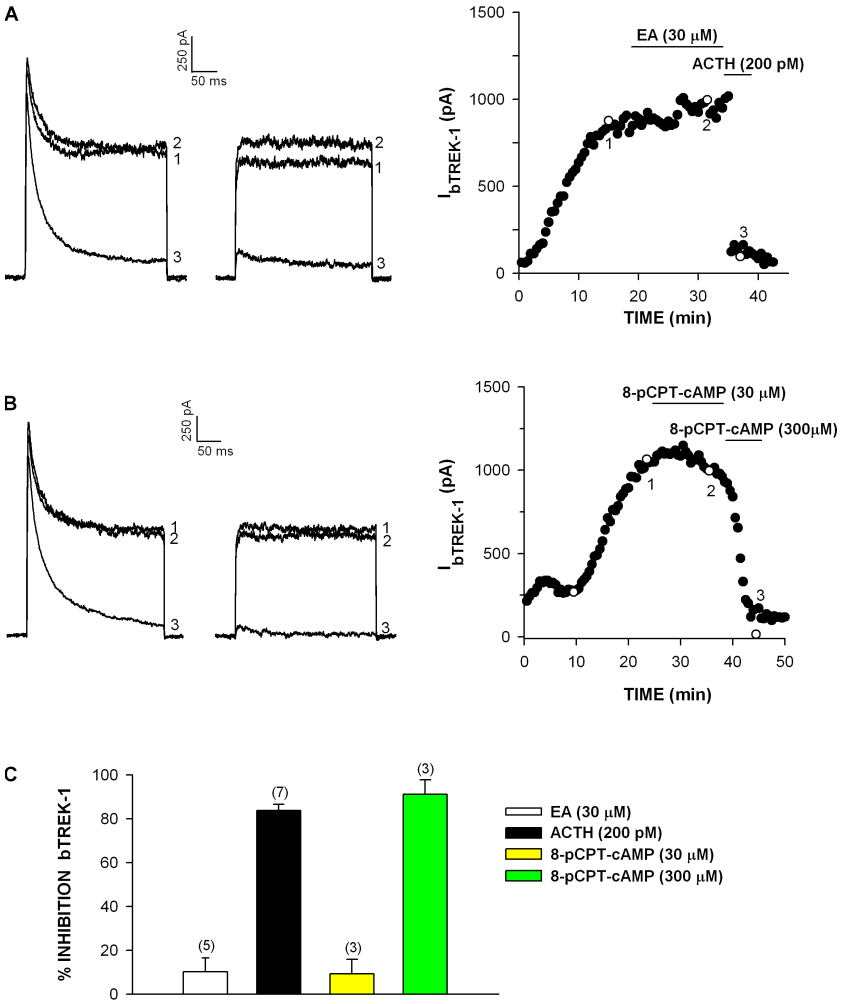


**Figure 5.** Effect of 8-pCPT-cAMP on bTREK-1 currents in perforated patch recordings. (A and B) Perforated patch recordings: whole cell $K^+$ currents were recorded in the nystatin perforated patch configuration in response to voltage steps applied at 30-s intervals from a holding potential of −80 to +20 mV with (right traces) or without (left traces) depolarizing prepulses. After bTREK-1 reached a stable amplitude, cells were superfused with 8-pCPT-2'-O-Me-cAMP (designated EA for Epac activator) (30 μM), ACTH (200 pM), or 8-pCPT-cAMP (30 or 300 μM), as indicated. Numbers on current traces correspond to those on plot at right. (C) Summary of experiments as in A and B. Bars indicate mean ± SEM of indicated number of determinations.

applied directly to the cytoplasm through the pipette. When applied through the pipette at concentrations from 1 to 30 μM, 8-pCPT-2'-O-Me-cAMP potently and effectively suppressed the time-dependent growth of bTREK-1 with an $IC_{50}$ of 0.63 μM (Fig. 6, A–D). Notably, at a concentration of 1 μM, 8-pCPT-2'-O-Me-cAMP reduced bTREK-1 current density by 63.7% from a control value of 45.2 ± 5.9 pA/pF ($n$ = 15) to 16.4 ± 4.4 pA/pF ($n$ = 6). Using this low concentration of 8-pCPT-2'-O-Me-cAMP in the pipette, bTREK-1 amplitude initially grew, but then declined to a steady-state value (Fig. 6 B). At higher concentrations, the initial increase in bTREK-1 amplitude was absent and inhibition of bTREK-1 activity was nearly complete (Fig. 6, C and D). The inhibition of bTREK-1 expression by 8-pCPT-2'-O-Me-cAMP was specific. This agent did not alter the expression of the voltage-gated Kv1.4 current in these cells (Fig. 6 E).

When applied intracellularly through the patch pipette, 8-pCPT-2'-O-Me-cAMP inhibited bTREK-1 at concentrations similar to those that activate Epac in vitro ($EC_{50}$ = 2.2 μM). By comparison, 10–20-fold higher concentrations were required to activate PKA holoenzyme (Enserink et al., 2002). Accordingly, we found that 8-pCPT-2'-O-Me-cAMP activated PKA in AZF cell lysates only at concentrations significantly higher than those required to inhibit bTREK-1 current (Fig. 7 C).

### Inhibition of bTREK-1 by 8-pCPT-2′-O-Me-cAMP Is Independent of PKA

The suppression of bTREK-1 expression in AZF cells by 8-pCPT-2'-O-Me-cAMP at concentrations that induce little or no activation of PKA indicate that this enzyme does not mediate the inhibition. Accordingly, 8-pCPT-2'-O-Me-cAMP was effective in inhibiting bTREK-1 activity in the presence of PKA antagonists.

In the experiments illustrated in Fig. 7 (A and B), AZF cells were preincubated for at least 30 min with the cell-permeable PKA inhibitor myristolyated PKI(14–22) amide (4 μM) and H-89 (5 or 10 μM) before recording $K^+$ currents with pipettes containing PKI(6–22) amide (4 μM) and H-89 (5 or 10 μM) with no further addition or with 8-pCPT-2'-O-Me-cAMP at several concentrations. The PKA inhibitors failed to suppress bTREK-1 inhibition by 8-pCPT-2'-O-Me-cAMP at concentrations from 5 to 30 μM (Fig. 7, A and B). In contrast, when PKI(6–22) amide and H-89 were added to AZF cell cytoplasmic extracts,

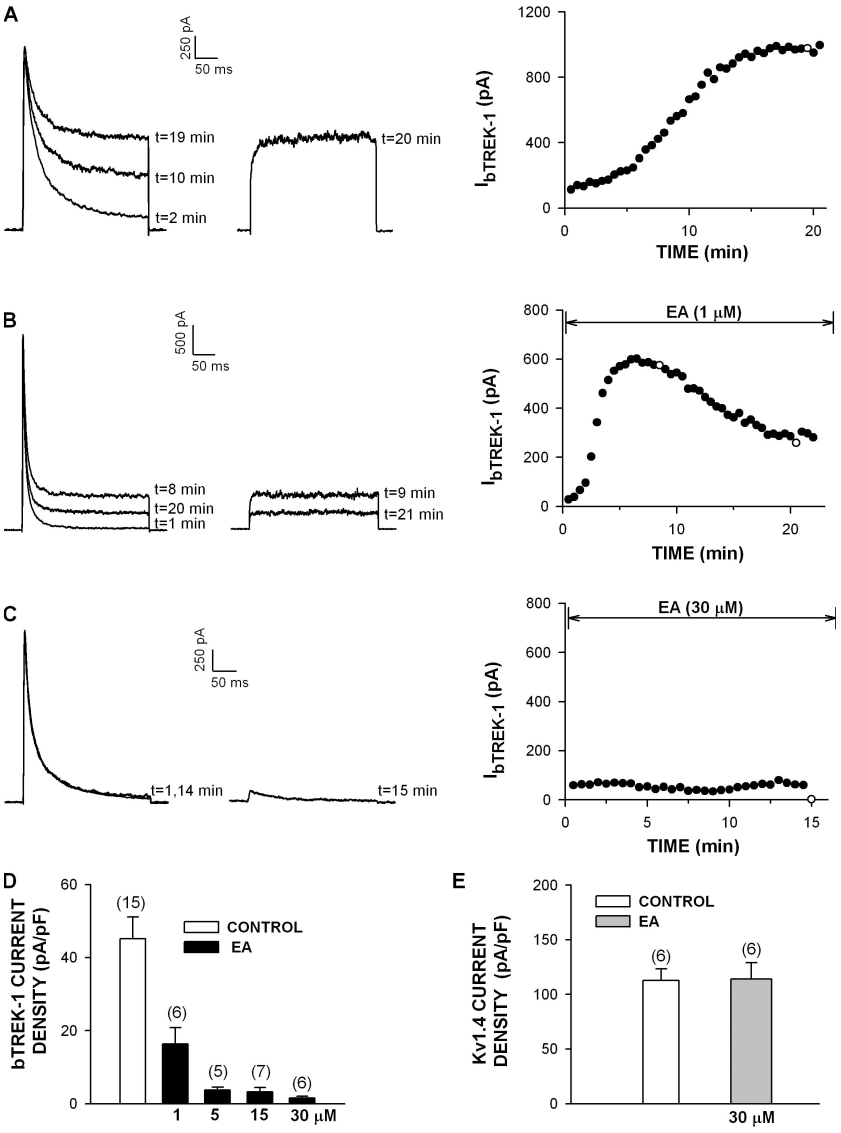


**Figure 6.** Concentration-dependent inhibition of bTREK-1 by 8-pCPT-2'-O-Me-cAMP. $K^+$ currents were recorded from AZF cells with standard pipette solution or the same solution supplemented with 8-pCPT-2'-O-Me-cAMP (EA) at concentrations from 1 to 30 μM. Currents were recorded in response to voltage steps to +20 mV applied at 30-s intervals from a holding potential of −80 mV with and without depolarizing prepulses. (A–C) Time-dependent increase in bTREK-1 and inhibition by 8-pCPT-2'-O-Me-cAMP (EA). Current traces recorded with (right) and without (left) depolarizing prepulses at indicated times. bTREK-1 amplitudes are plotted at right. Open circles indicate traces recorded with depolarizing prepulse. (D) Summary of experiments as in A–C. Bars indicate bTREK-1 current density in pA/pF expressed as the mean ± SEM of the indicated number of determinations. (E) Effect of 8-pCPT-2'-O-Me-cAMP (EA) on Kv1.4 current. Bars indicate Kv1.4 current density in pA/pF expressed as the mean ± SEM of the indicated number of determinations in control saline and in the presence of 8-pCPT-2'-O-Me-cAMP (30 μM) (EA).

PKA activation by 8-pCPT-2'-O-Me-cAMP (1–30 μM) or cAMP (5 μM) was completely inhibited to levels below control values (Fig. 7 C). Overall, 8-pCPT-2'-O-Me-cAMP effectively suppressed bTREK-1 channel activity under conditions where PKA had been completely eliminated.

Adenosine-3′-5′-cyclic monophosphorothioate, Rp isomer (Rp-cAMPS) competitively inhibits cAMP activation of PKA, but not Epac, in living cells (Holz et al., 2008; Poppe et al., 2008). The presence of 500 μM Rp-cAMPS in the pipette solution failed to blunt the complete inhibition of bTREK-1 by 8-pCPT-2'-O-Me-cAMP (30 μM), providing further evidence for an Epac2-dependent inhibition of bTREK-1 (Fig. 7, A and D).

### Inhibition of bTREK-1 by 8-pCPT-2′-O-Me-cAMP Requires Hydrolyzable ATP

The inhibition of bTREK-1 by ACTH and 8-pCPT-cAMP requires hydrolyzable ATP (Enyeart et al., 1996). If 8-pCPT-2'-O-Me-cAMP–mediated inhibition of bTREK-1 also proceeds through an ATP hydrolysis-dependent mechanism, then substitution of the nonhydrolyzable ATP analogue AMP-PNP for ATP in the pipette solution should eliminate inhibition by the Epac2 activator. Accordingly, when pipette solutions contained 2 mM AMP-PNP in place of ATP, 8-pCPT-2'-O-Me-cAMP (30 μM) failed to suppress bTREK-1 expression in whole cell recordings (Fig. 7 D).

### Inhibition of bTREK-1 in Twice Patched Cells by 8-pCPT-2′-O-Me-cAMP

In whole cell recordings, intracellularly applied 8-pCPT-2'-O-Me-cAMP suppressed bTREK-1 expression, even when the AZF cell had been preincubated with PKA inhibitors, and the patch electrode contained PKA inhibitors. To further demonstrate that 8-pCPT-2'-O-Me-cAMP inhibited bTREK-1 under conditions where PKA activity had been totally blocked in advance, AZF cells were sequentially patched with a pipette containing the PKA

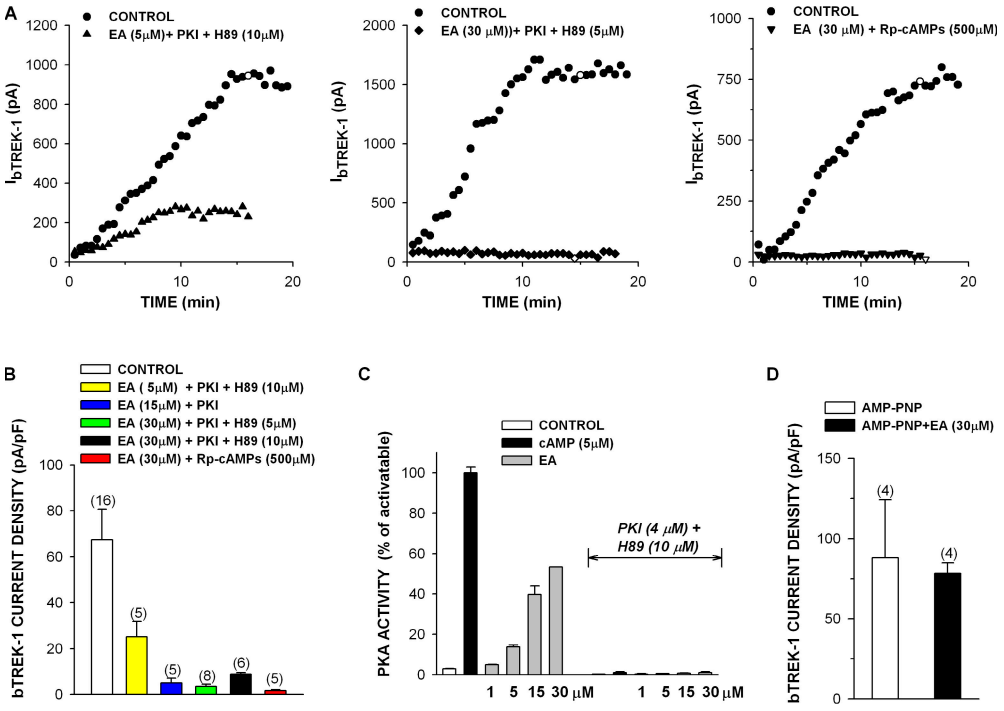


**Figure 7.** bTREK-1 inhibition by 8-pCPT-2'-O-Me-cAMP is independent of PKA. (A–C) Whole cell $K^+$ currents were recorded in response to voltage steps applied at 30-s intervals from −80 to +20 mV with or without depolarizing prepulses. Pipettes contained standard solution or the same solution supplemented with 8-pCPT-2'-O-Me-cAMP (EA), either alone or in combination with PKA inhibitors H-89 (10 μM), PKI(6–22) amide (4 μM), and Rp-cAMPS (500 μM), as indicated. When pipettes contained PKA inhibitors H-89 and PKI(6–22), cells were also pretreated for 30 min with H-89 (10 μM) and myristolated PKI(14–22) peptide (4 μM) before initiating recording. (A) Plots of bTREK-1 amplitude against time with pipettes containing indicated solutions. (B) Summary of experiments as in A. Bars indicate bTREK-1 current density in pA/pF expressed as the mean ± SEM of the indicated number of determinations. (C) Effect of 8-pCPT-2'-O-Me-cAMP (EA) and PKA inhibitors on PKA activity in AZF cell lysates: PKA activity was determined in cell lysates after incubating AZF cells either without (untreated) or with PKA inhibitors for 30 min. PKA activity in lysates from untreated cells was measured after 5 min with no further addition (control) or after addition of cAMP (5 μM) or 8-pCPT-2'-O-Me-cAMP (1–30 μM) (EA). PKA activity in lysates from PKA inhibitor–treated cells was measured after 5 min incubation with cAMP (5 μM) or 8-pCPT-2'-O-Me-cAMP (1–30 μM) (EA) and the PKA inhibitors as indicated. PKA activity is expressed as % of that activatable by 5 μM cAMP in control lysates. (D) Effect of AMP-PNP on 8-pCPT-2'-O-Me-cAMP inhibition of bTREK-1 current. bTREK-1 current was measured at 30-s intervals using patch pipettes containing AMP-PNP (2 mM) in place of ATP, or this same solution plus 8-pCPT-2'-O-Me-cAMP (30 μM) (EA). Bars represent mean ± SEM of maximum current density for the indicated number of determinations.

antagonists, followed by one containing these antagonists as well as 8-pCPT-2'-O-Me-cAMP.

Control experiments showed that AZF cells could often be consecutively patched with two pipettes without compromising the recording of bTREK-1 currents. In the experiment illustrated in Fig. 8 A, the cell was consecutively patched by two pipettes containing standard pipette solution. bTREK-1 current amplitude remained relatively constant upon voltage clamping the cell with the second pipette. In contrast, when the second pipette contained 8-pCPT-2'-O-Me-cAMP (15 μM), bTREK-1 was rapidly inhibited (Fig. 8 B). Similar results were obtained in each of four experiments.

Finally, when cells were first voltage clamped with pipettes containing PKI (4 μM) and H-89 (10 μM) to preinhibit PKA, subsequent voltage clamp of the cell with patch electrodes containing the PKA inhibitors as well as 8-pCPT-2'-O-Me-cAMP produced near complete inhibition of bTREK-1 (Fig. 8 C).

### 8-pCPT-2′-O-Me-cAMP Fails to Inhibit bTREK-1 when Epac2 Expression Is Suppressed by ACTH

In a previous study, we demonstrated that prolonged treatment of AZF cells with ACTH enhances the expression of bTREK-1 mRNA and $K^+$ channels (Enyeart et al., 2003). We now report that, under similar conditions, ACTH markedly suppresses the expression of Epac2 mRNA. In the experiment illustrated in Fig. 9 A, AZF cells were treated with ACTH (2 nM) for 48 h before isolating mRNA. Northern analysis showed that Epac2-specific mRNA was markedly reduced, compared with its time-matched control.

When AZF cells were exposed to ACTH (10 nM) for 72 or 96 h before recording $K^+$ currents, 8-pCPT-2'-O-Me-cAMP failed to inhibit bTREK-1 expression. In the experiments illustrated in Fig. 9 B, $K^+$ currents were recorded from ACTH-treated cells with pipettes containing either standard solution plus PKA inhibitors, or the same solution supplemented with 8-pCPT-2'-O-Me-cAMP (5 μM). The maximum bTREK-1 current densities were nearly identical in the absence or presence of the Epac activator. In contrast, when $K^+$ currents were recorded from ACTH-treated cells using pipettes containing 8-br-cAMP, which activates PKA as well as Epac2, bTREK-1 was nearly completely inhibited (Fig. 9 B).

In other experiments, AZF cells were treated for 72–96 h with ACTH (10 nM) before patch clamping them with pipettes containing PKA inhibitors followed by

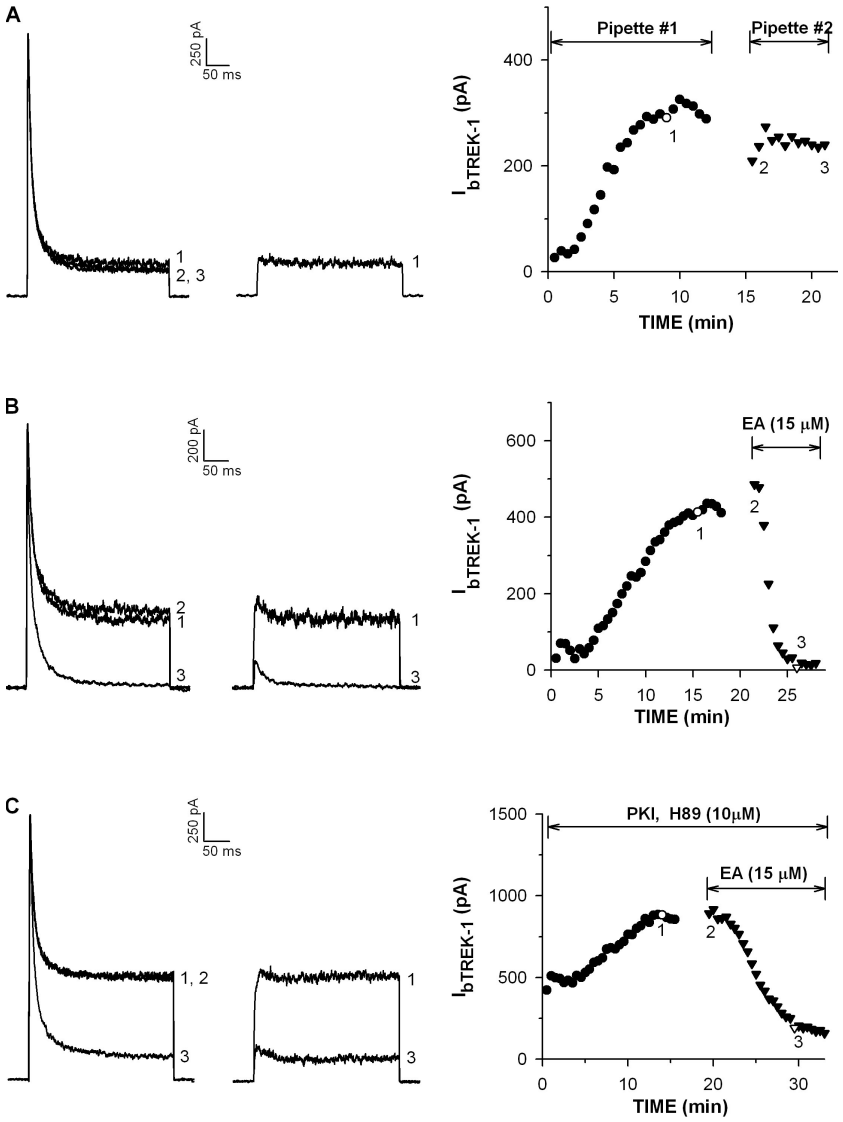


**Figure 8.** Inhibition of bTREK-1 by 8-pCPT-2'-O-Me-cAMP in twice-patched cells. Whole cell $K^+$ currents were recorded in response to voltage steps to +20 mV applied at 30-s intervals from −80 mV, with or without depolarizing prepulses. Cells were sequentially patched with two pipettes containing standard solution, or the same solution supplemented with PKI(6–22) amide (4 μM), H-89 (10 μM), or 8-pCPT-2'-O-Me-cAMP (EA) as indicated. When bTREK-1 reached a stable maximum, the first pipette was withdrawn and the cell patched again with the second pipette. (A–C) Current traces and corresponding plots of bTREK-1 amplitude against time for cells patch clamped with pipettes containing the additions indicated. Closed circles represent pipette #1, closed triangles, pipette #2. Numbers on traces at left correspond to those on plot at right. Break in graph denotes time required to change patch pipettes.

PKA inhibitors plus 8-pCPT-2'-O-Me-cAMP (5 μM). Under these conditions, 8-pCPT-2'-O-Me-cAMP (5 μM) failed to produce any inhibition of bTREK-1 current in each of four cells (Fig. 9 C). In fact, maximum bTREK-1 density was slightly increased from 26.1 ± 3.0 to 29.6 ± 7.9 pA/pF in the presence of the Epac activator. In contrast, when the experiment was repeated with cells that had not been pretreated with ACTH, 8-pCPT-2'-O-Me-cAMP inhibited bTREK-1 by 88.1 ± 3.1% ($n = 4$) (Fig. 9 D).

### 8-pCPT-2′-O-Me-cAMP Does Not Inhibit bTREK-1 Activity in Transfected HEK293 Cells

Epac2 is robustly expressed in a limited number of tissues, including the adrenal glands of rats and humans (Kawasaki et al., 1998). However, the distribution of Epac2 expression within the adrenal has not been determined. Specifically, it hasn't been shown that Epac2 is expressed in adrenal cortical cells, rather than neural crest–derived adrenal chromaffin cells. In Northern blots of mRNA from bovine AZF cells, Epac2 was readily detected. By comparison, little or no Epac2 mRNA could be detected in HEK293 cells (Fig. 10 D). Experiments were done to determine whether 8-pCPT-2'-O-Me-cAMP could inhibit the activity of cloned bTREK-1 channels expressed in HEK293 cells where Epac2 is poorly expressed. In contrast to its effect in bovine AZF cells, the presence of 8-pCPT-2'-O-Me-cAMP in the pipette solution at 5 or 15 μM failed to alter the functional expression of bTREK-1 in transfected HEK293 cells (Fig. 10, A and C).

Although Epac2 may be absent from HEK293 cells, these cells do express functional PKA (Rich et al., 2007). N6-benzoyl-cAMP (6-Bnz-cAMP) is a cAMP analogue that selectively activates PKA over Epac (Christensen et al., 2003). When 6-Bnz-cAMP (15 μM) was included in the pipette solution, the activity of transfected bTREK-1 $K^+$ channels in HEK293 cells was markedly suppressed from a control value of 141.2 ± 25.8 pA/pF ($n = 19$) to 34.5 ± 6.4 pA/pF ($n = 9$) (Fig. 10, B and D). These results

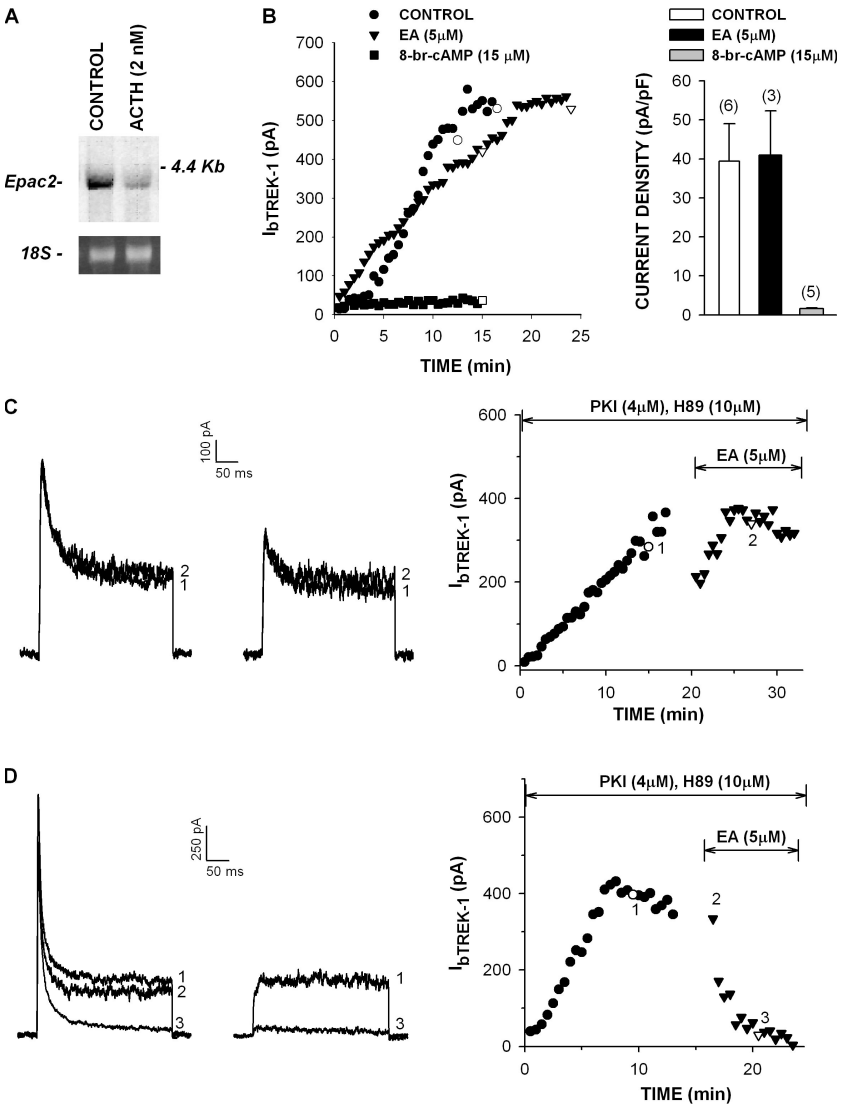


**Figure 9.** Effect of suppression of Epac2 expression on bTREK-1 inhibition by 8-pCPT-2'-O-Me-cAMP and 8-br-cAMP. (A) Northern blot analysis of ACTH inhibition of Epac2 mRNA expression. AZF cells were cultured either without (control) or with ACTH (2nM). mRNA was isolated after 48 h and analyzed as described in Materials and methods. (B) 8-pCPT-2'-O-Me-cAMP and bTREK-1 expression in ACTH-treated cells. AZF cells were exposed to ACTH (10 nM) for 72–96 h before patch clamping with pipettes containing PKI amide (6–22) (4 μM) and H89 (10 μM) (control), this same solution supplemented with 8-pCPT-2'-O-Me-cAMP (5 μM) (EA), or a solution containing 8-br-cAMP (15 μM). bTREK-1 current amplitudes are plotted against time. Bar graphs: summary of bTREK-1 maximum current densities. Values are mean ± SEM of indicated number of determinations. (C and D) Effect of ACTH treatment on bTREK-1 inhibition by 8-pCPT-2'-O-Me-cAMP in twice-patched cells. AZF cells were cultured in serum-supplemented media with (C) or without (D) 10 nM ACTH for 72–96 h before sequentially recording $K^+$ currents with pipettes containing PKI amide (6–22) (4 μM) plus H89 (10 μM) and then these two agents plus 8-pCPT-2'-O-Me-cAMP (EA) (5 μM). $K^+$ current traces recorded with (right traces) and without (left traces) depolarizing prepulses. Numbers on traces correspond to those on plots of bTREK-1 amplitude at right.

show that 8-pCPT-2'-O-Me-cAMP fails to inhibit bTREK-1 activity in cells that poorly express Epac2, while these same channels are inhibited in response to specific activation of PKA.

## DISCUSSION

The major findings of this study are that ACTH, NPS-ACTH, and cAMP inhibit bTREK-1 $K^+$ channels in bovine AZF cells by multiple cAMP-dependent signaling pathways that likely involve the activation of both PKA and Epac2. bTREK-1 is among the first $K^+$ channels identified thus far that is inhibited by parallel cAMP-dependent pathways. ATP-sensitive $K^+$ channels of pancreatic β cells are also inhibited by cAMP through separate PKA- and Epac-dependent mechanisms (Light et al., 2002; Kang et al., 2008). The convergent inhibition of bTREK-1 $K^+$ channels by these two cAMP-dependent mechanisms provides for efficient fail-safe depolarization of AZF cells by ACTH.

### PKA-independent Inhibition of bTREK-1 by ACTH and Forskolin

Experiments in which PKI(6–22) amide and H-89 failed to blunt bTREK-1 inhibition by ACTH or forskolin provide convincing evidence that inhibition of this channel by cAMP can occur through a PKA-independent mechanism. PKI(6–22) amide was used at concentrations ~1,000–2,000 times the reported $IC_{50}$ of 1.7 nM (Glass et al., 1989). H-89, which competes with ATP for its binding site on PKA, was used at 100–200 times its reported $IC_{50}$ of <50 nM (Hidaka et al., 1991). When applied together to AZF cell cytoplasmic extracts, these agents eliminated the activation of PKA by 8-pCPT-2'-O-Me-cAMP or cAMP. When applied together to the cytoplasm through the pipette solution, these agents should have completely blocked PKA activation by ACTH and forskolin, yet bTREK-1 inhibition was not affected.

The voltage-independent inhibition of bTREK-1 by ACTH and 8-pCPT-cAMP in the presence of PKA antagonists provided additional evidence that this response

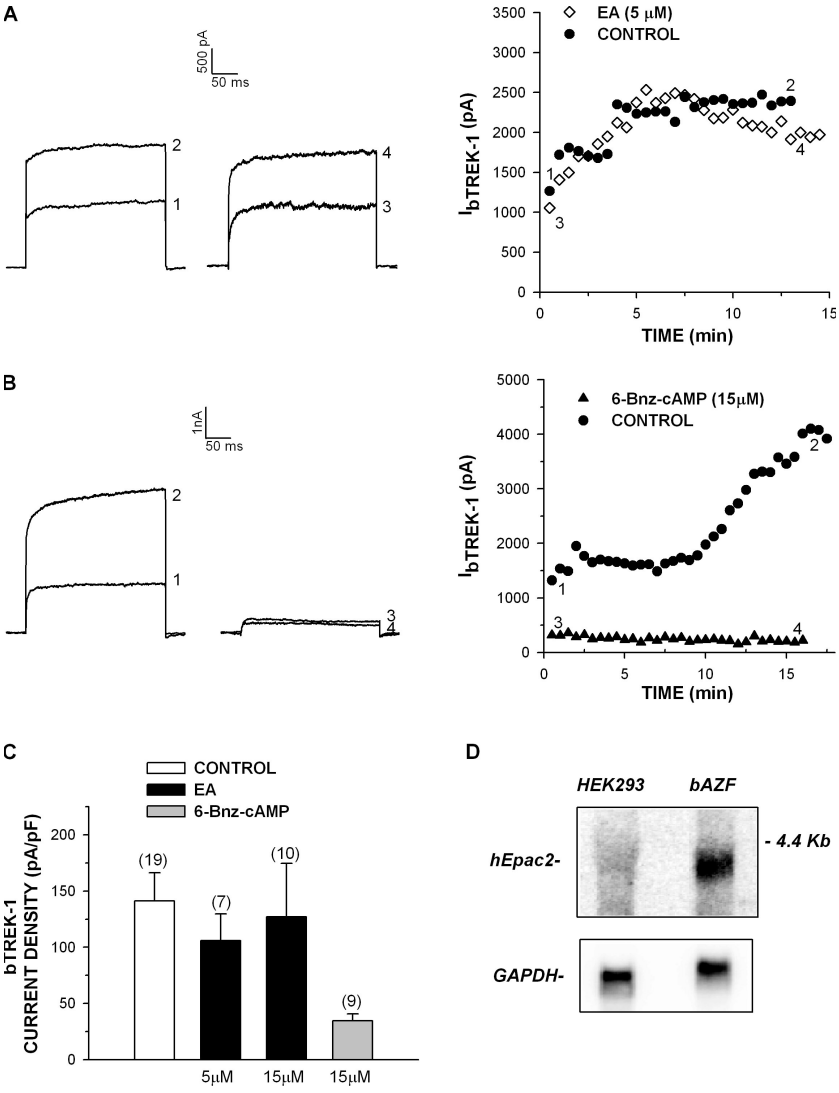


**Figure 10.** 6-Bnz-cAMP but not 8-pCPT-2'-O-Me-cAMP inhibits bTREK-1 channels expressed in HEK293 cells. Whole cell $K^+$ currents were recorded from HEK293 cells that had been transiently transfected with pCR3.1 uni-bTREK-1 cDNA. $K^+$ currents were activated by voltage steps to +20 mV, applied at 30-s intervals from a holding potential of −80 mV. Patch pipettes contained control saline or this same solution supplemented with 8-pCPT-2'-O-Me-cAMP (5 or 15 μM) (EA) or 6-Bnz-cAMP (15 μM). (A and B) Effect of 8-pCPT-2'-O-Me-cAMP (EA) and 6-Bnz-cAMP on bTREK-1 current. bTREK-1 current traces and associated time-dependent plots of current amplitudes. Numbers on traces correspond to those on plots at right. (C) Summary of experiments as shown in A and B. Bars indicate maximum bTREK-1 current density expressed as pA/pF. Values are mean ± SEM for indicated number of determinations. (D) Northern blot analysis of Epac2 in bovine AZF and HEK293 cells. Lanes contained 7 μg of poly(A)$^+$ RNA from the indicated cells. Hybridization with hEpac2 probe was performed as described in Materials and methods.

was not mediated through PKA. Previous studies showed that inhibition of neuronal TREK-1 channels by PKA-dependent phosphorylation occurred through a rightward shift in the voltage-dependent activation of these channels (Bockenhauer et al., 2001; Maingret et al., 2002). Consequently, open probability was not reduced at positive test voltages. In AZF cells, bTREK-1 was effectively inhibited by ACTH and 8-pCPT-cAMP regardless of test potential, suggesting the involvement of a separate PKA-independent mechanism.

### $Ca^{2+}$- and PKA-independent Inhibition of bTREK-1 by NPS-ACTH

NPS-ACTH reversibly inhibited bTREK-1 current with an $IC_{50}$ of 20 pM. Although this peptide was reported to trigger step-like and repetitive spike-like increases in $[Ca^{2+}]_i$ in bovine AZF cells (Yamazaki et al., 1998), it failed to inhibit bTREK-1 through a $Ca^{2+}$-dependent pathway similar to that activated by AngII. In this regard, AngII-stimulated increases in $[Ca^{2+}]_i$ are mediated mainly by $Ca^{2+}$ released from intracellular sites, while ACTH-mediated increases in $[Ca^{2+}]_i$ occur in response to $Ca^{2+}$ influx through voltage-gated $Ca^{2+}$ channels (Yamazaki et al., 1998; Hunyady and Catt, 2005). In whole-cell patch clamp experiments where cells are voltage clamped at −80 mV, ACTH-stimulated influx through voltage-gated channels would be eliminated, preempting a $Ca^{2+}$-dependent inhibition of bTREK-1. Under physiological conditions, $Ca^{2+}$ entry through voltage-gated channels could contribute to ACTH-stimulated bTREK-1 inhibition and membrane depolarization.

NPS-ACTH did increase the concentration of cAMP in AZF cells to a level sufficient to activate PKA. However, similar to ACTH, the inhibition of bTREK-1 by NPS-ACTH appeared not to be mediated by PKA. First, NPS-ACTH inhibited bTREK-1 half-maximally at a concentration 16-fold lower than that required for half-maximal activation of PKA. Second, TREK-1 inhibition by NPS-ACTH was insensitive to PKA inhibitors. Overall, these results are consistent with a mechanism where,

similar to ACTH, NPS-ACTH can inhibit bTREK-1 by a PKA-independent action of cAMP.

### Inhibition of bTREK-1 by 8-pCPT-2′-O-Me-cAMP

8-pCPT-2'-O-Me-cAMP potently and effectively inhibited bTREK-1 activity when applied intracellularly through the patch pipette in whole cell recordings. Several lines of evidence strongly indicate that this inhibition was mediated through Epac2. First, bTREK-1 expression was inhibited half-maximally with an $IC_{50}$ of <1 μM. This result is in excellent agreement with that reported for the potency of this agent in activating Epac1 and Epac2, where binding affinities and $EC_{50}$s of 1–5 μM have been reported (Enserink et al., 2002; Bos, 2003; Rehmann et al., 2003). In contrast, 8-pCPT-2'-O-Me-cAMP activates PKA only at 10–20-fold higher concentrations, and is far less effective than cAMP in this respect (Enserink et al., 2002; Bos, 2003).

Further, we showed that 8-pCPT-2'-O-Me-cAMP inhibited bTREK-1 completely at concentrations that produced little or no measurable increase in PKA activity in AZF cells. This agent also effectively inhibited bTREK-1 activity in cells where PKA had been inhibited by preincubating cells with PKA inhibitors and with these inhibitors included in the patch pipette at concentrations 100–1,000 times their reported $EC_{50}$s. Third, 8-pCPT-2'-O-Me-cAMP inhibited bTREK-1 in twice-patched cells where PKA was first preinhibited by direct application of the two PKA inhibitors to the cytoplasm through the patch pipette. Finally, 8-pCPT-2'-O-Me-cAMP was ineffective at inhibiting bTREK-1 channels when Epac2 expression had been suppressed by prolonged exposure of AZF cells to ACTH, or in HEK293 cells that express little or no Epac2. In contrast, cAMP derivatives that activate PKA retained their effectiveness in these two systems.

It isn't known whether cAMP might also inhibit bTREK-1 in other cells through PKA- and Epac2-dependent signaling pathways. Since the expression of Epac2 is limited, other cells expressing both Epac2 and bTREK-1 have not yet been identified. It is possible that TREK-1 inhibition through Epac2 could occur in selected CNS neurons that express both of these proteins.

### Signaling Mechanism for bTREK-1 Inhibition by 8-pCPT-2′-O-Me-cAMP

The mechanism by which 8-pCPT-2'-O-Me-cAMP inhibits bTREK-1 $K^+$ channels after activation of Epac2 is unknown. This Epac-selective cAMP analogue inhibits $K_{ATP}$ $K^+$ channels of pancreatic β cells and cell lines through an Epac2-dependent mechanism, wherein activated Epac2 interacts with the sulfonylurea receptor 1, a subunit of this inwardly rectifying $K^+$ channel to reduce channel activity (Kang et al., 2006). Further, it has recently been shown that Epac-selective cAMP activators function by sensitizing $K_{ATP}$ $K^+$ channels to inhibition by ATP, shifting the $IC_{50}$ 20-fold (Kang et al., 2008). bTREK-1 inhibition by this Epac-selective cyclic nucleotide occurs through a different mechanism, since inhibition is blocked when AMP-PNP replaces ATP in the pipette solution, indicating a requirement for ATP hydrolysis. Specific protein kinases activated by Epac2 have not been identified.

The failure of membrane-permeable 8'-substituted cAMP derivatives, including 8-pCPT-cAMP and 8-pCPT-2'-O-Me-cAMP to inhibit bTREK-1 when superfused externally at low concentrations in perforated patch recordings was unexpected. In perforated patch recording, whole cell dialysis is presumably limited when compared with standard whole cell recording. In standard whole cell recording, we previously found that 8-pCPT-cAMP inhibited bTREK-1 channels with an $IC_{50}$ of 167 μM, a concentration much higher than that required to activate PKA in intact AZF cells (Enyeart et al., 1996). Similar high concentrations of 8-pCPT-cAMP were also required to inhibit bTREK-1 in perforated patch recordings.

It seems likely that the reduced potency of cyclic nucleotides applied externally in perforated patch recordings stems from limited transport across the cell membrane. Their potency as bTREK-1 inhibitors increased markedly when they were directly applied to the cytoplasm through the patch pipette. Similar results have been seen in a study of the inhibition of $K_{ATP}$ $K^+$ channels by Epac-selective cAMP analogues in pancreatic β cells (Kang et al., 2006).

Overall, the selectivity of 8-pCPT-2'-O-Me-cAMP as an Epac-specific activator may have been overstated in the initial studies of this and similar compounds (Enserink et al., 2002; Christensen et al., 2003; Rehmann et al., 2003). It is clear that when applied externally to intact cells at concentrations >50 μM, these agents produce significant activation of PKA and possibly other cAMP-activated proteins. Results obtained from experiments where these agents were used at concentrations of 100 μM or more in the absence of PKA inhibitors should be interpreted with caution.

Although we have found that bovine AZF cells express Epac2 and that an Epac-selective cAMP analogue inhibits bTREK-1 at low concentrations under conditions where PKA is inhibited, and fails to inhibit bTREK-1 in cells when Epac2 expression has been suppressed, the possibility remains that 8-pCPT-2'-O-Me-cAMP inhibits bTREK-1 through a cAMP-binding protein different than PKA or Epac2. PKA- and Epac-independent actions of cAMP have been observed in neurons and endocrine cells (Ivins et al., 2004; Gambaryan et al., 2006).

Our results demonstrate that ACTH inhibits bTREK-1 $K^+$ channels in bovine AZF cells through activation of multiple cAMP-dependent signaling pathways. The convergent inhibition of bTREK-1 through separate PKA- and Epac2-dependent signaling pathways provides an efficient, reliable mechanism for membrane depolarization and $Ca^{2+}$ entry.

The inhibition of bTREK-1 by parallel cAMP-dependent pathways resembles that for AngII inhibition of these same channels by separate $Ca^{2+}$- and ATP hydrolysis–dependent pathways (Enyeart et al., 2005; Liu et al., 2007). In both instances, nature has developed fail-safe mechanisms for corticosteroid secretion in response to stress by activation of multiple convergent signaling pathways leading to membrane depolarization.

This work was supported by National Institutes of Health grant R01-DK47875 (to J.J. Enyeart).

Olaf S. Andersen served as editor.

Submitted: 20 March 2008
Accepted: 8 July 2008

## REFERENCES

Awad, J.A., R.A. Johnson, K.H. Jakobs, and G. Schultz. 1983. Interactions of forskolin and adenylate cyclase. Effects on substrate kinetics and protection against inactivation by heat and N-ethylmaleimide. *J. Biol. Chem.* 258:2960–2965.

Bockenhauer, D., N. Zilberberg, and S.A. Goldstein. 2001. KCNK2: reversible conversion of a hippocampal potassium leak into a voltage-dependent channel. *Nat. Neurosci.* 4:486–491.

Bos, J.L. 2003. Epac: a new cAMP target and new avenues in cAMP research. *Nat. Rev. Mol. Cell Biol.* 4:733–738.

Brooks, S.P., and K.B. Storey. 1992. Bound and determined: a computer program for making buffers of defined ion concentrations. *Anal. Biochem.* 201:119–126.

Buckley, D.I., and J. Ramachandran. 1981. Characterization of corticotropin receptors on adrenocortical cells. *Proc. Natl. Acad. Sci. USA.* 78:7431–7435.

Christensen, A.E., F. Sleheim, J. de Rooij, S. Dremier, F. Schwede, K. Dao, A. Martinez, C. Maenhaut, J.L. Bos, H.G. Genieser, and S.O. Doskeland. 2003. cAMP analog mapping of Epac1 and cAMP kinase. Discriminating analogs demonstrate that Epac and cAMP kinase act synergistically to promote PC-12 cell neurite extension. *J. Biol. Chem.* 278:35394–35402.

de Rooij, J., F.J. Zwartkruis, M.H. Verheijen, R.H. Cool, S.M. Nijman, A. Wittinghofer, and J.L. Bos. 1998. Epac is a Rap1 guanine-nucleotide-exchange factor directly activated by cyclic AMP. *Nature.* 396:474–477.

Enserink, J.M., A.E. Christensen, J. de Rooij, M. van Triest, F. Schwede, H.G. Genieser, S.O. Doskeland, J.L. Blank, and J.L. Bos. 2002. A novel Epac-specific cAMP analogue demonstrates independent regulation of Rap1 and ERK. *Nat. Cell Biol.* 4:901–906.

Enyeart, J.J., and J.A. Enyeart. 1998. Activation of separate calcium and A-kinase-dependent pathways by ACTH. *Endocr. Res.* 24:325–334.

Enyeart, J.J., B. Mlinar, and J.A. Enyeart. 1993. T-type $Ca^{2+}$ channels are required for ACTH-stimulated cortisol synthesis by bovine adrenal zona fasciculata cells. *Mol. Endocrinol.* 7:1031–1040.

Enyeart, J.J., B. Mlinar, and J.A. Enyeart. 1996. Adrenocorticotropic hormone and cAMP inhibit noninactivating $K^+$ current in adrenocortical cells by an A-kinase-independent mechanism requiring ATP hydrolysis. *J. Gen. Physiol.* 108:251–264.

Enyeart, J.J., J.C. Gomora, L. Xu, and J.A. Enyeart. 1997. Adenosine triphosphate activates a noninactivating $K^+$ current in adrenal cortical cells through nonhydrolytic binding. *J. Gen. Physiol.* 110:679–692.

Enyeart, J.A., L. Xu, and J.J. Enyeart. 2000. A bovine adrenocortical Kv1.4 $K^+$ channel whose expression is potently inhibited by ACTH. *J. Biol. Chem.* 275:34640–34649.

Enyeart, J.J., L. Xu, S. Danthi, and J.A. Enyeart. 2002. An ACTH- and ATP-regulated background $K^+$ channel in adrenocortical cells is TREK-1. *J. Biol. Chem.* 277:49186–49199.

Enyeart, J.A., S.J. Danthi, and J.J. Enyeart. 2003. Corticotropin induces the expression of TREK-1 mRNA and $K^+$ current in adrenocortical cells. *Mol. Pharmacol.* 64:132–142.

Enyeart, J.J., S.J. Danthi, H. Liu, and J.A. Enyeart. 2005. Angiotensin II inhibits bTREK-1 $K^+$ channels in adrenocortical cells by separate $Ca^{2+}$- and ATP hydrolysis-dependent mechanisms. *J. Biol. Chem.* 280:30814–30828.

Gambaryan, S., E. Butt, P. Tas, A. Smolenski, B. Allolio, and U. Walter. 2006. Regulation of aldosterone production from zona glomerulosa cells by ANG II and cAMP: evidence for PKA-independent activation of CaMK by cAMP. *Am. J. Physiol. Endocrinol. Metab.* 290:E423–E433.

Glass, D.B., L.J. Lundquist, B.M. Katz, and D.A. Walsh. 1989. Protein kinase inhibitor-(6-22)-amide peptide analogs with standard and nonstandard amino acid substitutions for phenylalanine 10. Inhibition of cAMP-dependent protein kinase. *J. Biol. Chem.* 264:14579–14584.

Gomora, J.C., and J.J. Enyeart. 1998. $Ca^{2+}$ depolarizes adrenal cortical cells through selective inhibition of an ATP-activated $K^+$ current. *Am. J. Physiol.* 275:C1526–C1537.

Grahame-Smith, D.G., R.W. Butcher, R.L. Ney, and E.W. Sutherland. 1967. Adenosine 3′,5′-monophosphate as the intracellular mediator of the action of adrenocorticotropic hormone on the adrenal cortex. *J. Biol. Chem.* 242:5535–5541.

Hamill, O.P., A. Marty, E. Neher, B. Sakmann, and F.J. Sigworth. 1981. Improved patch clamp techniques for high resolution current recording from cells and cell-free membrane patches. *Pflugers Arch.* 391:85–100.

Haynes, R.C. Jr., S.B. Kortitz, and F.G. Peron. 1959. Influence of adenosine 3′,5′-monophosphate on corticoid production by rat adrenal glands. *J. Biol. Chem.* 234:1421–1423.

Haynes, R.C.J., and L. Berthet. 1957. Studies on the mechanism of action of the adrenocorticotropic hormone. *J. Biol. Chem.* 225:115–124.

Hidaka, H., M. Watanabe, and R. Kobayashi. 1991. Properties and use of H-series compounds as protein kinase inhibitors. *In* Methods in Enzymology. Vol. 201. Academic Press, Inc., Orlando, FL. 328–339.

Holz, G.G., O.G. Chepurny, and F. Schwede. 2008. Epac-selective cAMP analogs: new tools with which to evaluate the signal transduction properties of cAMP-regulated guanine nucleotide exchange factors. *Cell. Signal.* 20:10–20.

Honoré, E. 2007. The neuronal background K2P channels: focus on TREK1. *Nat. Rev. Neurosci.* 8:251–261.

Horn, R., and A. Marty. 1988. Muscarinic activation of ionic currents measured by a new whole-cell recording method. *J. Gen. Physiol.* 92:145–159.

Hunyady, L., and K.J. Catt. 2005. Pleiotropic $AT_1$ receptor signaling pathways mediating physiological and pathogenic actions of angiotensin II. *Mol. Endocrinol.* 20:953–970.

Ivins, J.K., M.K. Parry, and D.A. Long. 2004. A novel cAMP-dependent pathway activates neuronal integrin function in retinal neurons. *J. Neurosci.* 24:1212–1216.

Jurman, M.E., L.M. Boland, Y. Liu, and G. Yellen. 1994. Visual identification of individual transfected cells for electrophysiology using antibody-coated beads. *Biotechniques.* 17:876–881.

Kang, G., O.G. Chepurny, B. Malester, M.J. Rindler, H. Rehmann, J.L. Bos, F. Schwede, W.A. Coetzee, and G.G. Holz. 2006. cAMP sensor Epac as a determinant of ATP-sensitive potassium channel activity in human pancreatic β cells and rat INS-1 cells. *J. Physiol.* 573:595–609.

Kang, G., C.A. Leech, O.G. Chepurny, W.A. Coetzee, and G.G. Holz. 2008. Role of the cAMP sensor Epac as a determinant of $K_{ATP}$ channel ATP sensitivity in human pancreatic β-cells and rat INS-1 cells. *J. Physiol.* 586:1307–1319.

Kawasaki, H., G.M. Springett, N. Mochizuki, S. Toki, M. Nakaya, M. Matsuda, D.E. Housman, and A.M. Graybiel. 1998. A family of cAMP-binding proteins that directly activate Rap1. *Science.* 282:2275–2279.

Kimoto, T., Y. Ohta, and S. Kawato. 1996. Adrenocorticotropin induces calcium oscillations in adrenal fasciculata cells: single cell imaging. *Biochem. Biophys. Res. Commun.* 221:25–30.

Light, P.E., J.E. Manning Fox, M.J. Riedel, and M.B. Wheeler. 2002. Glucagon-like peptide-1 inhibits pancreatic ATP-sensitive potassium channels via a protein kinase A- and ADP-dependent mechanism. *Mol. Endocrinol.* 16:2135–2144.

Liu, H., J.A. Enyeart, and J.J. Enyeart. 2007. Angiotensin II inhibits native bTREK-1 $K^+$ channels through a PLC-, kinase C-, and PIP2-independent pathway requiring ATP hydrolysis. *Am. J. Physiol. Cell Physiol.* 293:C682–C695.

Maingret, F., E. Honore, M. Lazdunski, and A.J. Patel. 2002. Molecular basis of the voltage-dependent gating of TREK-1, a mechano-sensitive $K^+$ channel. *Biochem. Biophys. Res. Commun.* 292:339–346.

Mlinar, B., B.A. Biagi, and J.J. Enyeart. 1993. A novel $K^+$ current inhibited by ACTH and angiotensin II in adrenal cortical cells. *J. Biol. Chem.* 268(12):8640–8644.

Mlinar, B., and J.J. Enyeart. 1993. Voltage-gated transient currents in bovine adrenal fasciculata cells II: A-type $K^+$ current. *J. Gen. Physiol.* 102:239–255.

Moyle, W.R., Y.C. Kong, and J. Ramachandran. 1973. Steroidogenesis and cyclic adenosine 3′,5′-monophosphate accumulation in rat adrenal cells. *J. Biol. Chem.* 248(7):2409–2417.

Patel, A.J., E. Honore, F. Maingret, F. Lesage, M. Fink, F. Duprat, and M. Lazdunski. 1998. A mammalian two pore domain mechano-gated S-like $K^+$ channel. *EMBO J.* 17:4283–4290.

Penhoat, A., C. Jaillard, and J.M. Saez. 1989. Corticotropin positively regulates its own receptors and cAMP response in cultured bovine adrenal cells. *Proc. Natl. Acad. Sci. USA.* 86:4978–4981.

Poppe, H., S.D. Rybalkin, H. Rehmann, T.R. Hinds, X.B. Tang, A.E. Christensen, F. Schwede, H.G. Genieser, J.L. Bos, S.O. Doskeland, et al. 2008. Cyclic nucleotide analogs as probes of signaling pathways. *Nat. Methods.* 5:277–278.

Raikhinstein, M., M. Zohar, and I. Hanukoglu. 1994. cDNA cloning and sequence analysis of the bovine adrenocorticotropic hormone (ACTH) receptor. *Biochim. Biophys. Acta.* 1220:329–332.

Rehmann,H., B.Prakash, E.Wolf, A.Rueppel, J. de Rooij, J.L. Bos, and A. Wittinghofer. 2003. Structure and regulation of the cAMP-binding domains of Epac2. *Nat. Struct. Biol.* 10:26–32.

Rich, T.C., W. Xin, C. Mehats, K.A. Hassell, L.A. Piggott, X. Le, J.W. Karpen, and M. Conti. 2007. Cellular mechanisms underlying prostaglandin-induced transient cAMP signals near the plasma membrane of HEK-293 cells. *Am. J. Physiol. Cell Physiol.* 292:C319–C331.

Richardson, M.C., and D. Schulster. 1973. The role of protein kinase activation in the control of steroidogenesis by adrenocorticotrophic hormone in the adrenal cortex. *Biochem. J.* 136:993–998.

Roesler, W.J., G.R. Vandenbark, and R.W. Hanson. 1988. Cyclic AMP and the induction of eukaryotic gene transcription. *J. Biol. Chem.* 263:9063–9066.

Sala, G.B., K. Hayashi, K.J. Catt, and M.L. Dufau. 1979. Adrenocorticotropin action in isolated adrenal cells. The intermediate role of cyclic AMP in stimulation of corticosterone synthesis. *J. Biol. Chem.* 254:3861–3865.

Simpson, E.R., and M.R. Waterman. 1988. Regulation of the synthesis of steroidogenic enzymes in adrenal cortical cells by ACTH. *Annu. Rev. Physiol.* 50:427–440.

Waterman, M.R. 1994. Biochemical diversity of cAMP-dependent transcription of steroid hydroxylase genes in the adrenal cortex. *J. Biol. Chem.* 269:27783–27786.

Yamazaki, T., T. Kimoto, K. Higuchi, Y. Ohta, S. Kawato, and S. Kominami. 1998. Calcium ion as a second messenger for *o*-nitrophenylsufenyl-adrenocorticotropin (NPS-ACTH) and ACTH in bovine adrenal steroidogenesis. *Endocrinology.* 139:4765–4771.

Yanagibashi, K., M. Kawamura, and P.F. Hall. 1990. Voltage-dependent $Ca^{2+}$ channels are involved in regulation of steroid synthesis by bovine but not rat fasciculata cells. *Endocrinology.* 127:311–318.